INSTITUTE OF PHYSICS PUBLISHING JOURNAL OF PHYSICS: CONDENSED MATTER

J. Phys.: Condens. Matter **16** (2004) 9243–9258 PII: S0953-8984(04)86269-6

Ni intercalation of titanium diselenide: effect on the lattice, specific heat and magnetic properties

N V Baranov[1,2,5], K Inoue[3], V I Maksimov[1,2], A S Ovchinnikov[2], V G Pleschov[2], A Podlesnyak[4], A N Titov[1] and N V Toporova[2]

[1] Institute of Metal Physics, Ekaterinburg 620219, Russia
[2] Ural State University, Lenin Av. 51, Ekaterinburg 620083, Russia
[3] Institute for Molecular Science, Myodaiji, Okazaki 444, Japan
[4] Laboratory for Neuron Scattering, ETH Zürich and PSI, Villigen PSI CH-5232, Switzerland

E-mail: nikolai.baranov@usu.ru

Received 16 September 2004
Published 3 December 2004
Online at stacks.iop.org/JPhysCM/16/9243
doi:10.1088/0953-8984/16/50/014

Abstract

Intercalated Ni_xTiSe_2 compounds with Ni concentration up to $x = 0.5$ have been investigated using x-ray diffraction, magnetic susceptibility and specific heat measurements. A set of peculiarities caused by the intercalation, such as a significant decrease of the gap between Se–Ti–Se trilayers and depletion of the low-frequency phonons due to the stiffening of the lattice as well as an enhancement of the density of electronic states at low Ni content ($x < 0.33$), is attributed to hybridization of the Ni 3d states with $TiSe_2$ bands and formation of covalent-like links between Se–Ti–Se trilayers via the inserted Ni ions. Ni_xTiSe_2 compounds with intercalant content up to $x = 0.5$ show a paramagnetic behaviour unlike M_xTiSe_2 compounds intercalated by other 3d metals (M = Cr, Mn, Fe, Co). The Ni magnetic moment in Ni_xTiSe_2 is suggested to be of an itinerant nature. A pronounced correlation between the change of the lattice parameter c_0 and the value of the effective magnetic moment, which is observed in Ni_xTiSe_2 as well in M_xTiSe_2 systems intercalated by other 3d metals, indicates that the magnetic moment on the inserted atom is controlled by the hybridization degree of M 3d states with $TiSe_2$ bands.

1. Introduction

Titanium dichalcogenides TiX_2 (X = S, Se, Te), which have a layered crystal structure, have been the subject of numerous investigations because of their interesting properties; at the same time, they are very important as parent compounds for intercalation materials [1, 2]. The main feature of TiX_2 is a weak coupling between X–Ti–X trilayers via van der Waals forces.

[5] Address for correspondence: Chair of Condensed Matter Physics, Ural State University, Ekaterinburg, Russia.

By the insertion of various guest M atoms into van der Waals gaps, a wide class of M_xTiX_2 compounds with new interesting physical properties can be obtained. The main goal of the intercalation is to synthesize materials with new functions. Among the parent compounds, much attention has been paid to the study of $TiSe_2$ which exhibits a charge density wave (CDW) at $T < T_t \sim 200$ K [1–4]. The phase transition of $TiSe_2$ to a commensurate superlattice ($2 \times 2 \times 2$) with a decrease in temperature below T_t was studied by various methods including the measurement of neutron diffraction [4, 5], ultrasonic velocity [6], specific heat [7] and electrical [4] and optical [8] properties. Different models such as Fermi surface nesting [4, 9], the excitonic insulator model [10] and the band Jahn–Teller effect [11] were proposed during the last few decades to explain the CDW transition in this compound. Recent re-examinations of $TiSe_2$ by synchrotron x-ray diffuse scattering experiments [12] and by angle-resolved photoemission with high resolution [13] have shown that the CDW transition in this compound obviously originates from electron–hole coupling together with the indirect Jahn–Teller effect, whereas, according to [14], the phonon softening observed in $TiSe_2$ in the vicinity of T_t [12] may also be explained within a model of the antiferroelectric instability.

Many works were devoted to the study of TiX_2 compounds intercalated by 3d-transition (M) metals. A small amount of M atoms inserted between X–Ti–X trilayers is found to suppress the formation of CDW in $TiSe_2$. The intercalation of 3d metals significantly modifies the lattice, electrical and magnetic properties of TiX_2 [1, 2, 15–18]. The guest M atoms usually occupy the octahedrally coordinated sites in the van der Waals gaps, resulting in contraction or expansion of the averaged interlayer distance, depending on the type of M metal and its concentration, while the intralayer spacing changes insignificantly upon intercalation. According to the band structure calculations performed for some ordered M_xTiX_2 (X = S, Se) compounds, the 3d-electron states of M ions are hybridized with TiX_2 bands [1, 18, 19]. Photoelectron spectroscopy studies performed for M_xTiS_2 [20, 21] and M_xTiSe_2 [22] systems have indeed revealed a strong hybridization of M 3d states with Ti 3d and X 3(4)p states. Moreover, the appearance of a narrow band near the Fermi level in M_xTiSe_2 compounds with M = Cr and Co [22] is observed, in comparison with the parent compound $TiSe_2$. Some indication of a growth of the density of electronic states (DOS) at E_F, owing to the formation of such bands at the intercalation, was obtained by magnetic susceptibility [17, 23–25] and specific heat measurements [26, 27] and by spectroscopy studies [20–22].

Of the M_xTiX_2 family members, the magnetic properties were more extensively studied for M_xTiS_2 compounds. The existence of different magnetic states ranging from paramagnetism and spin-glass-like behaviour to states with three-dimensional magnetic order was established in TiS_2 intercalated by V, Cr, Mn, Fe, Co and Ni [28–32]. The magnetic state of these compounds was found to depend on the type and concentration of the 3d element intercalated between the X–Ti–X layers. The long-range ferromagnetic order with the easy axis parallel to the *c*-axis was observed in Fe_xTiS_2 at $x > 0.4$ [30]. The magnetic properties of the M_xTiSe_2 family are significantly less well investigated and the data presented in the different works seem to be contradictory. Thus, the magnetic susceptibility measurements performed in [17] for M_xTiSe_2 with M = V, Cr, Mn, Fe, Co, Ni and Cu at $x = 0.1$ and 0.2 have revealed that all these compounds are paramagnets above 4.2 K, while in other works [23, 24, 33] it has been shown that the M_xTiSe_2 compounds with M = Cr, Mn and Fe exhibit a spin-glass or cluster-glass behaviour within the concentration range $0 < x \leqslant 0.2$. Such a discrepancy may result from a difference in the sample preparation. At a higher M content ($x \geqslant 0.25$), long-range antiferromagnetic order was revealed in Fe_xTiSe_2 by neutron diffraction investigations [16], in contrast to the ferromagnetism of the Fe_xTiS_2 compounds. An antiferromagnetic-like behaviour was also observed in $Cr_{0.5}TiSe_2$ by magnetization and susceptibility measurements [23]. The effective magnetic moments μ_{eff} found in the literature for the 3d metals in M_xTiSe_2 are

significantly smaller than the ionic values [17, 23, 24]. Such a reduction in μ_{eff} is ascribed to the hybridization of the M 3d states with $TiSe_2$ bands as in the M_xTiS_2 family [17].

Systematic study of the concentration dependence of magnetic properties has been performed for relatively few M_xTiSe_2 systems. In particular, for M = Cr, Fe and Mn [23, 24, 33], it has been shown that the intercalation leads not only to a reach variety of magnetic states in a low temperature range but also causes an appreciable change of the μ_{eff} value depending on the type and content of M atoms. This behaviour clearly indicates that the M 3d–Ti 3d hybridization degree in M_xTiSe_2 depends on the atomic number of the 3d metal as in M_xTiS_2 compounds. Since there is a lack of data concerning the Ni intercalation in the literature, the present work studies the x-ray diffraction, magnetic susceptibility and specific heat of Ni_xTiSe_2 compounds in order to achieve an extended view of the effects of the 3d-metal intercalation on the main physical properties of $TiSe_2$.

2. Experimental details

Polycrystalline Ni_xTiSe_2 samples ($0 < x \leqslant 0.5$) were prepared by an ampoule synthesis method from the constituent elements. The starting materials were Ti (99.9), Se (99.99) and Ni (99.9). The method of synthesis included several stages. At first, the parent compound $TiSe_2$ was synthesized by heat treatment of a mixture of the starting materials Ti and Se at 900 °C for 150 h. At the second stage, the mixture of Ni and $TiSe_2$ powders was pressed into cylinder pellets, sealed in evacuated quartz tubes and annealed at 800 °C for 1 week. The lower temperature of the second stage was chosen in order to prevent the substitution of Ni atoms for Ti atoms in the $TiSe_2$ matrix. The obtained specimens were milled, compacted into pellets and then homogenized under the same conditions for 1 week. Bearing in mind possible positional arrangements of Ni atoms within a layer at the intercalation [34], the samples were quenched from 800 °C by dropping the tubes into water in order to obtain samples with a random distribution of Ni atoms among accessible sites in the van der Waals gaps. Powder x-ray diffraction patterns were obtained using a DRON-4-13 diffractometer with Co K_α radiation. Crystal structure refinements were performed using a full-profile method (the GSAS program [35]). The unit cell parameters were determined with an accuracy of $\Delta a_0 = \pm 0.001$ Å and $\Delta c_0 = \pm 0.002$ Å.

The dc magnetic susceptibility was measured by means of a Quantum Design SQUID magnetometer in the temperature interval from 2–300 K. Specific heat measurements were performed using PPMS (Quantum Design, USA) on 5–10 mg pieces of compacted powder samples.

3. Results

3.1. Crystal structure

As is seen in figure 1, the x-ray diffraction patterns for those Ni_xTiSe_2 compounds with Ni concentration up to $x = 0.33$ do not show any additional peaks which may be associated with either superlattice structure owing to the positional arrangement of Ni atoms and vacancies or with the presence of foreign phases. The Ni-intercalated Ni_xTiSe_2 compounds with Ni content below $x = 0.33$ have the same hexagonal crystal structure of the CdI_2 type ($P\bar{3}m1$ space group) as the parent compound $TiSe_2$. The best fit of the experimental x-ray patterns is obtained when the intercalated atoms are situated in octahedral positions. The coordinates of the atoms in the unit cell are: Ti (0, 0, 0); Se (1/3, 2/3, z) and Ni (0, 0, 1/2). However, the insertion of Ni atoms into the van der Waals gap of $TiSe_2$ is found to significantly influence the lattice parameters

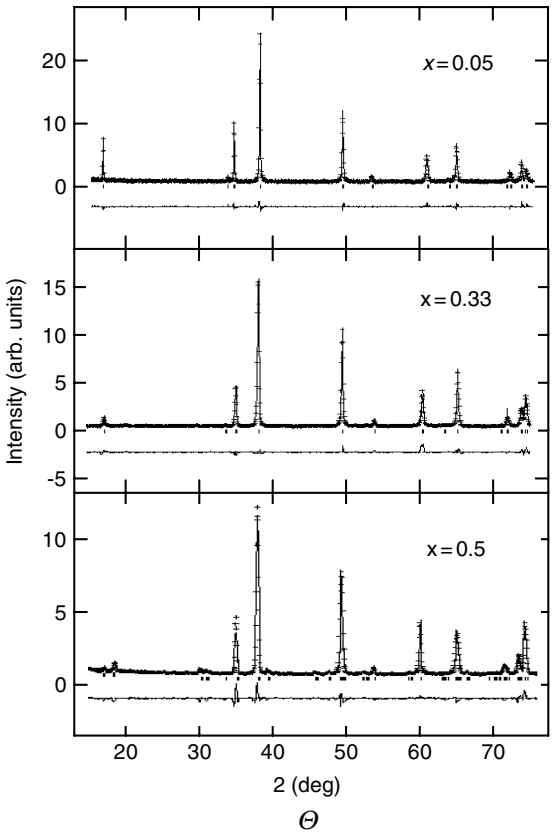

Figure 1. X-ray patterns for Ni_xTiSe_2 compounds with various Ni content at room temperature.

(see figure 2). The concentration dependence of the parameter c_0 shows a substantial decrease with an increase in x up to $x = 0.25$, while a further increase of the Ni content up to $x = 0.5$ results in a slight growth of the c_0 value. As for the parameter a_0, it increases monotonically with intercalation in the entire concentration range ($0 < x \leqslant 0.5$). It should be noted that the lattice contraction along the c_0-direction was observed over a low concentration range ($x \leqslant 0.25$) in M_xTiSe_2 compounds intercalated by other 3d metals (Cr, Fe, Co) except Mn [24, 33, 36]. The observed decrease in c_0 and the ratio c_0/a_0 at the intercalation may originate from both the lowering of the thickness of the Se–Ti–Se trilayer (r_L) and the reduction of the gap width (r_G) between trilayers. Variation of r_L and r_G values for the Ni_xTiSe_2 system at the intercalation is displayed in figure 3. As can be seen, the gap width significantly decreases with an increase in Ni content, while the r_L value remains practically constant for $0.05 \leqslant x \leqslant 0.33$. These data allow us to suggest that (i) the decrease of the gap width is the main reason for the lattice contraction of Ni_xTiSe_2 along the c-direction with an increase in x and (ii) the geometry of the Se surrounding of Ti atoms does not change appreciably at the intercalation.

An increase of the intercalant content above $x = 0.33$ leads to a change of the crystal structure as can be seen on examination of the x-ray diffraction pattern for $Ni_{0.5}TiSe_2$ (figure 1). The crystal structure of this compound may be described quite well (with $R_w = 6\%$) as being of a monoclinic type (space group I 2/m) with unit cell parameters $a_0 = 6.161(1)$ Å, $b_0 = 3.567(1)$ Å, $c_0 = 11.836(2)$ Å and $\beta = 90.29(3)^o$. This structure may result from the

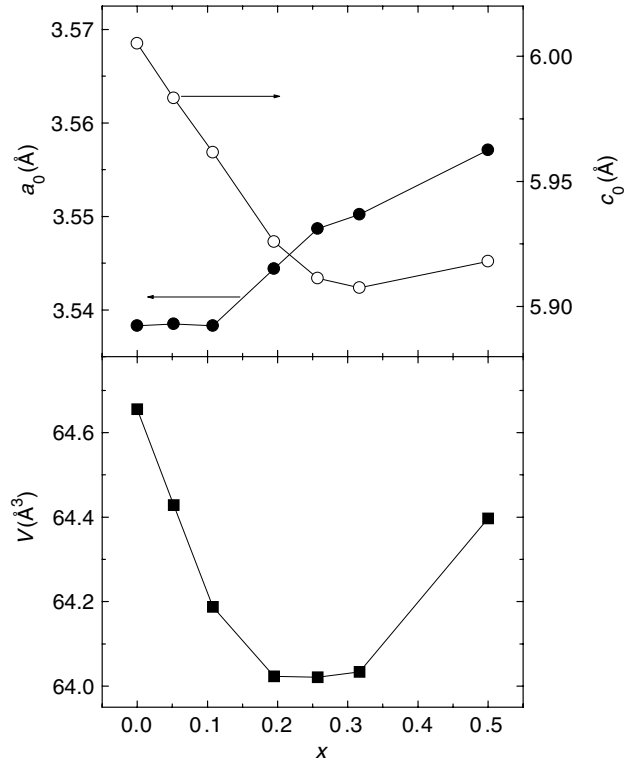

Figure 2. Variations of the lattice parameters a and c with the Ni concentration in Ni_xTiSe_2 compounds.

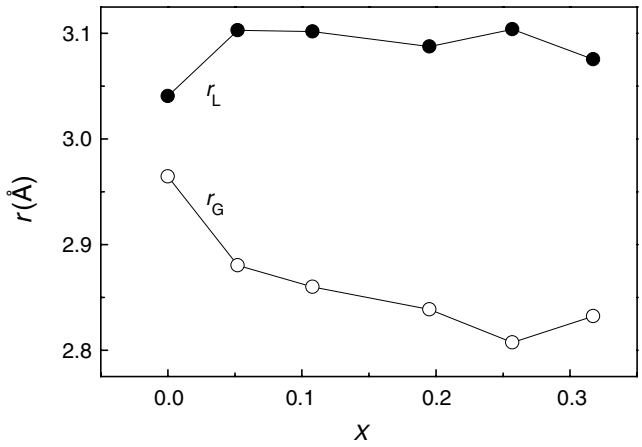

Figure 3. Concentration dependence of the thickness of the Se–Ti–Se trilayer and the width of the van der Waals gap in the Ni_xTiSe_2 system.

ordering of Ni atoms in a superlattice, $\sqrt{3}a_0 \times a_0 \times 2c_0$. The change in the crystal structure above $x = 0.33$ is accompanied by growth of the unit cell volume (figure 2(b)). It should be noted that the same kind of superstructure ($\sqrt{3}a_0 \times a_0 \times 2c_0$) caused by an ordering of intercalated Fe atoms and vacancies was found to exist at $x = 0.5$ in the Fe_xTiSe_2 series [37].

3.2. Magnetic susceptibility

Figure 4(a) displays the temperature dependences of the magnetic susceptibility for Ni_xTiSe_2 compounds. The susceptibility of the parent compound $TiSe_2$ reveals weak temperature dependence above ∼100 K and a low-temperature upturn of the Curie–Weiss (CW) type. At middle temperatures, the susceptibility has a negative sign, which is associated with the presence of the diamagnetic contribution from the ions with fully filled electron shells. After subtraction of the CW term from the $\chi(T)$ dependence for $TiSe_2$, one can observe an anomalous change of the contribution associated with paramagnetic behaviour of the conduction electrons (shown in the inset to figure 4(a)), i.e., the Pauli paramagnetic contribution χ_p. The critical temperature $T_t \approx 200$ K, at which a substantial reduction of the Pauli contribution occurs with a decrease in temperature, is associated with the appearance of the CDW. Our data for $TiSe_2$ are in good agreement with previous results [4]. As was suggested in [4], the presence of the low-temperature CW contribution to the total susceptibility of $TiSe_2$ may result from magnetic impurities.

The intercalation of Ni atoms into the van der Waals gaps of the $TiSe_2$ matrix is found to increase the low-temperature upturn and modify the high-temperature form of the susceptibility. According to our data, all Ni_xTiSe_2 compounds with Ni content up to $x = 0.5$ remain paramagnetic with decreasing temperature down to 2 K. The effect of the Ni intercalation is more clearly seen in figure 4(b) which displays the temperature dependence of the inverse susceptibility of the compounds with various Ni content. Thus, the temperature dependence of χ for Ni_xTiSe_2 is suggested to include two temperature-dependent contributions:

$$\chi(T) = \frac{C}{T - \theta_p} + \chi_0(T). \tag{1}$$

The first contribution in (1) is of the CW type, which dominates in the low-temperature region (<100 K), and the second term involves both the temperature-dependent Pauli paramagnetic contribution from conduction electrons and the diamagnetic contribution, i.e. $\chi_0(T) = \chi_p(T) + \chi_d$. Figure 4(c) shows the inverse susceptibility $(\chi - \chi_d)^{-1}$ for the parent $TiSe_2$ after subtraction of the temperature-independent diamagnetic contribution $\chi_d = 0.52 \times 10^{-6}$ emu g^{-1} Oe^{-1} [23] for comparison. The temperature dependences of the inverse susceptibility for Ni_xTiSe_2 show a pronounced non-monotonic character owing to the competition of two temperature-dependent contributions in (1), unlike the $\chi^{-1}(T)$ curves for the compounds intercalated by other 3d metals, which are nonlinear but monotonic above their ordering temperatures (see [23, 24], for example), since for M_xTiSe_2 (M = Cr, Fe, Mn, Co) the first term in (1) significantly surpasses the second one. As it turned out, the temperature dependence of the magnetic susceptibility of Ni_xTiSe_2 compounds may be described by the expression

$$\chi(T) = \frac{C}{T - \theta} + \chi_d + \chi_{p0} - PT^2, \tag{2}$$

where χ_{p0} and P are constants. The best-fitting results are presented in figure 4(b) (solid line). As can be seen, the experimental data agree with this expression quite well in the entire temperature interval; however, some discrepancy in the low-temperature range is observed for the compound with $x = 0.33$. Using equation (2), the effective magnetic moment μ_{eff}, paramagnetic Curie temperature θ_p, parameter P and the sum $(\chi_d + \chi_{p0})$ were determined for each compound. The last was obtained by extrapolation of the $\chi_0(T)$ curves presented in the inset to figure 4(a) to $T = 0$. All these data are collected in table 1. The effective magnetic moment per Ni ion in Ni_xTiSe_2 compounds is found to be significantly lower than $\mu_{eff}^{calc} = 2.83\mu_B$ for the free Ni^{2+} ion as was observed for M_xTiX_2 compounds intercalated by other 3d metals. The maximal value of $\mu_{eff} = 0.3\mu_B$ is obtained for $x = 0.1$; with further growth

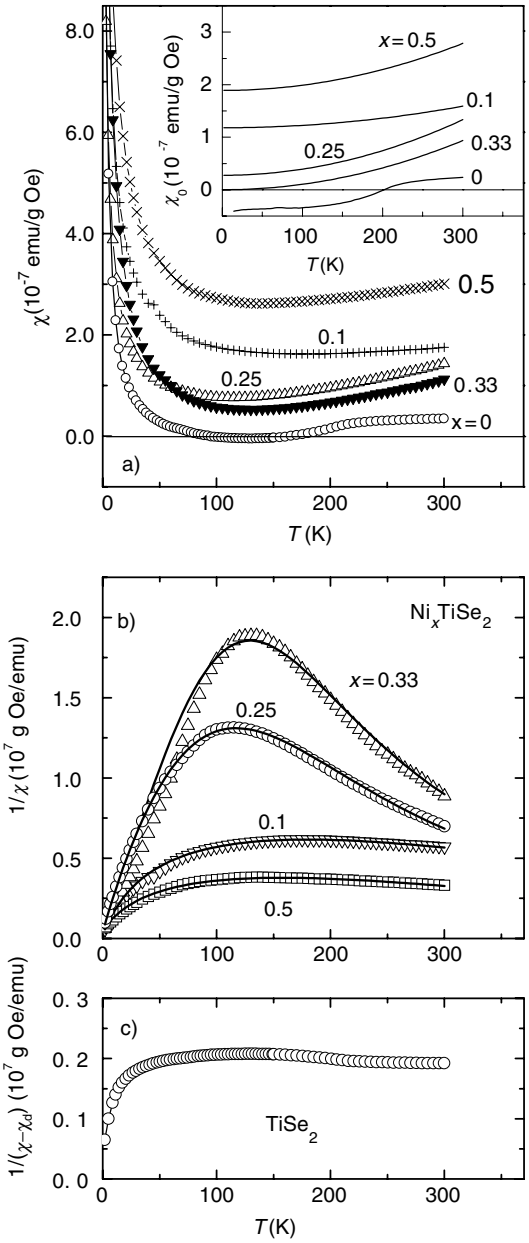

Figure 4. (a) Temperature dependence of the magnetic susceptibility of Ni_xTiSe_2 at various Ni content (inset shows the temperature dependence of χ_0 for Ni_xTiSe_2 after subtraction of the CW contribution from the total susceptibility); (b) χ^{-1} versus T curves for Ni-intercalated compounds (solid lines correspond to fitting by expression (2)); and (c) $(\chi-\chi_d)^{-1}$ versus T dependence for the parent compound $TiSe_2$.

of the Ni content, the value of $\mu_{\rm eff}$ decreases and remains almost unchanged ($0.16\mu_B-0.18\mu_B$) within the concentration range $0.25 \leqslant x \leqslant 0.5$. The θ_p of those compounds with Ni content $x \leqslant 0.33$ is estimated to be about -1 K, which implies an insignificance of the Ni–Ni exchange interaction over this concentration range. All values of $\mu_{\rm eff}$ presented in table 1 are slightly

Table 1. The effective magnetic moment $\mu_{\rm eff}$ per Ni atom, the paramagnetic Curie temperature $\theta_{\rm p}$, the sum $(\chi_{\rm d}+\chi_{\rm p0})$ of the diamagnetic and Pauli paramagnetic contributions to the total magnetic susceptibility (obtained by extrapolation of χ_0 to $T=0$), the coefficient P of the T^2 term in expressions (2) and (3) and the coefficient γ of the electronic contribution to the total specific heat, for Ni_xTiSe_2 compounds with various Ni content.

X	$\mu_{\rm eff}$ ($\mu_{\rm B}$)	$\theta_{\rm p}$ (K)	$\chi_{\rm d}+\chi_{\rm p0}$ (10^{-7} emu g^{-1} Oe^{-1})	P (K^{-2})	γ (mJ g-at.$^{-1}$ K^{-2})
0	–	–	−0.4	–	0.3
0.1	0.3	−1.3	1.2	-4.55×10^{-13}	–
0.25	0.17	−1.5	0.28	-1.18×10^{-12}	2.1
0.33	0.16	−1.0	∼0.00	-1.06×10^{-12}	1.4
0.5	0.18	−4.6	1.9	-9.94×10^{-13}	1.9

overestimated because we did not take into account the small contribution arising from impurities in the $TiSe_2$ matrix. Subtraction of the CW contribution caused by impurities in the parent compound $TiSe_2$ from the total susceptibility of Ni_xTiSe_2 leads to a decrease of the effective magnetic moment per Ni atom by about $0.05\mu_{\rm B}$. This value seems to be quite large for Ni_xTiSe_2 compounds because of the low values of $\mu_{\rm eff}$ for the Ni ion; nevertheless, we suppose that this additional contribution does not significantly influence the character of the concentration dependence of $\mu_{\rm eff}$, since in the present work we have used the same parent matrix $TiSe_2$ for the synthesis of all Ni-intercalated compounds.

As one can see from the inset to figure 4(a), the second contribution in (1), which was obtained after subtraction of the CW term, reveals gradual growth with an increase in temperature for all intercalated Ni_xTiSe_2 compounds as well as for $TiSe_2$. There are no indications of the appearance of CDW in the Ni_xTiSe_2, even at $x=0.1$. This result is in agreement with other studies [4, 23], which showed that the intercalation of d metals suppresses the superlattice formation in $TiSe_2$. As follows from estimations in [23], the diamagnetic contribution to the total magnetic susceptibility of M_xTiSe_2 should not change significantly upon intercalation. Therefore the change of χ_0 with the Ni content and with the temperature may be associated mainly with a change in the paramagnetic contribution from the conduction electrons $\chi_{\rm p}$. It should be noted that the pronounced temperature dependence of the magnetic susceptibility was found to exist in many d-transition metals that do not possess magnetic order [38]. Such a temperature dependence of $\chi_{\rm p}$ is associated with the change in the DOS value $N(E_{\rm F})$ at $E_{\rm F}$ and its first N' and second N'' derivatives [38]:

$$\chi_{\rm p}=\mu_{\rm B}^2N(E_{\rm F})\left\{1-\frac{\pi^2k_{\rm B}^2}{6}\left[\left(\frac{N'}{N}\right)^2-\left(\frac{N''}{N}\right)\right]_{E=E_{\rm F}}T^2\right\}=\chi_{\rm p0}-P\,T^2. \tag{3}$$

As follows from table 1, the intercalation of Ni is accompanied by a non-monotonic change of $\chi_0(T=0)=(\chi_{\rm d}+\chi_{\rm p0})$; at first (up to $x=0.1$), this value increases significantly and reaches the value $\sim1.2\times10^{-7}$ emu g^{-1} Oe^{-1} which agrees quite well with the Pauli contribution obtained for $Ni_{0.1}TiSe_2$ by Tazuke and Takeyama [17]. However, according to our data, the value of χ_0 increases with an increase in temperature, whereas, in [17], such a contribution was suggested to be temperature-independent. An increase of the Ni content up to $x=0.33$ is accompanied by lowering of $\chi_0(T=0)$, while further intercalation leads to the growth of $\chi_0(T=0)$ up to $\sim1.9\times10^{-7}$ emu g^{-1} Oe^{-1} at $x=0.5$. It should be mentioned that unlike Ni_xTiSe_2 compounds, for which an appreciable growth of χ_0 is observed, the paramagnetic contribution from conduction electrons to the total magnetic susceptibility of M_xTiSe_2 compounds intercalated

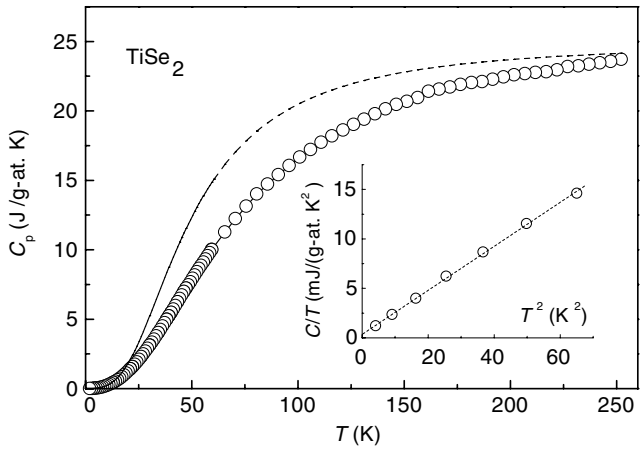

Figure 5. Temperature dependence of the specific heat for $TiSe_2$. The solid line corresponds to the lattice contribution calculated in the Debye model with $\Theta_D = 203$ K. Inset: C_p/T versus T^2 dependence.

by other 3d metals (M = Cr, Mn, Fe, Co) was suggested to be temperature-independent [23, 24, 33, 36]. In our opinion, the last may be caused by the fact that the temperature dependence of χ_0 is masked in this case by the large CW term and, therefore, cannot be revealed so distinctly as in the Ni_xTiSe_2 system.

3.3. Heat capacity

Figure 5 shows the temperature dependence of the specific heat for the parent compound $TiSe_2$. As it turned out, at low temperatures (<7 K), the C_p versus T curve can be well described by the well-known expression $C_p(T) = \gamma T + \beta T^3$ (see inset to figure 5). For the temperature interval 2–7 K, the electronic specific coefficient γ is estimated to be about 0.3 mJ g-at.$^{-1}$ K^{-2} and the Debye temperature Θ_D is found to be ∼203 K. Our γ value is larger than that obtained in [7] for a powder sample ($\gamma = 0.18$ mJ g-at.$^{-1}$ K^{-2}). Although the error in our estimation of γ is rather large due to the small γ value, such a discrepancy may be attributed to differences in the sample preparation. The low electronic contribution to the total specific heat of $TiSe_2$ is associated with the presence of the above-mentioned CDW state in this compound. Using the value $\Theta_D = 203$ K, we did not succeed in the description of the experimental $C_p(T)$ dependence over the entire temperature range (2–250 K). The increase in the specific heat of $TiSe_2$ above 7 K is more gradual than would be expected for a simple Debye model with a temperature-independent effective Debye temperature. This is clearly seen from figure 5, where the calculated lattice contribution for $\Theta_D = 203$ K is shown by the broken line. Our heat capacity measurements on the compacted powder sample of $TiSe_2$ did not reveal any anomaly around 200 K, which can be associated with the phase transition from the superlattice state with CDW to the normal state with increasing temperature, while such a transition was demonstrated by the measurements of the magnetic susceptibility (figure 4) and electrical resistivity [39] on the powder sample synthesized by the same method. It should be noted that a small anomaly of the specific heat at $T \approx 200$ K was observed in an earlier work [7] on a small single crystal with a mass of ∼0.3 mg.

Figure 6 displays the $C_p(T)$ dependences for Ni_xTiSe_2 in the temperature interval from 2–100 K. The low-temperature part of the $C_p(T)$ dependence for $x = 0$ is also presented in this

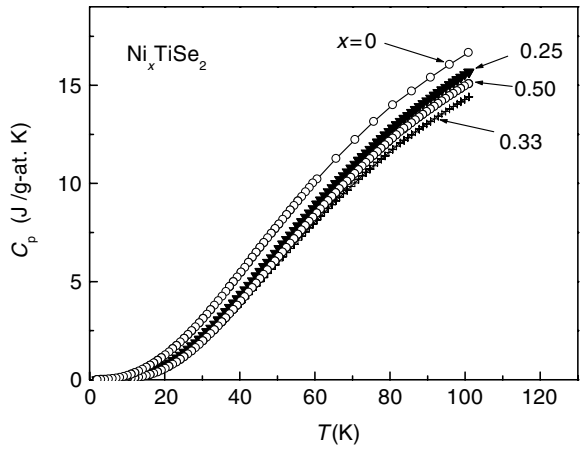

Figure 6. Temperature dependence of the specific heat for intercalated Ni_xTiSe_2 compounds.

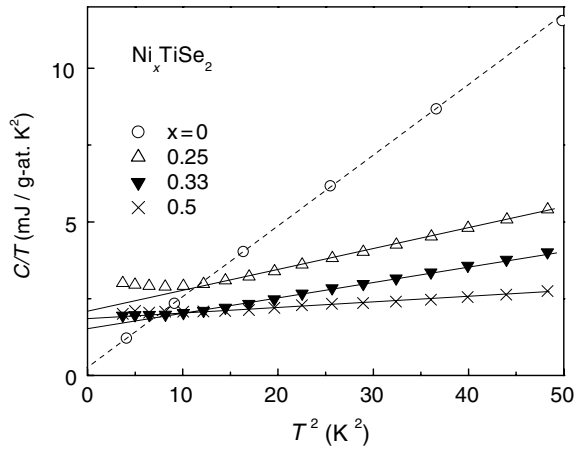

Figure 7. C_p/T versus T^2 for Ni_xTiSe_2 at various Ni content.

figure for comparison. As can be seen, the intercalation of Ni ions leads to appreciable change of the lattice contribution to the heat capacity. At first, the increase of the Ni concentration up to $x = 0.33$ decreases the lattice contribution, while further growth of the Ni content results in an increase of the lattice contribution. As in the case of the pure $TiSe_2$ compound, we could not describe the phonon contribution to the $C_p(T)$ dependences for Ni_xTiSe_2 in the Debye model with a temperature-independent value of Θ_D. In order to evaluate the electronic contribution to the specific heat, we plotted in figure 7 the C_p/T versus T^2 curves in the low-temperature region. The values of γ are presented in table 1. The intercalation of Ni up to $x = 0.25$ results in growth of the γ value. An enhancement of the γ value at the 3d-metal intercalation was also observed in M_xTiS_2 compounds [26]. However, within the M_xTiS_2 series, the growth of γ in the case of Ni intercalation is not so substantial as in the case of intercalation by other 3d metals. An analogous situation may be expected for M_xTiSe_2 systems. The increase of the Ni concentration above $x = 0.25$ leads to a non-monotonic change of γ within the interval 1.4–2.1 mJ g-at.$^{-1}$ K^{-2}. Another feature which can be seen in figure 7 is the flattening or small

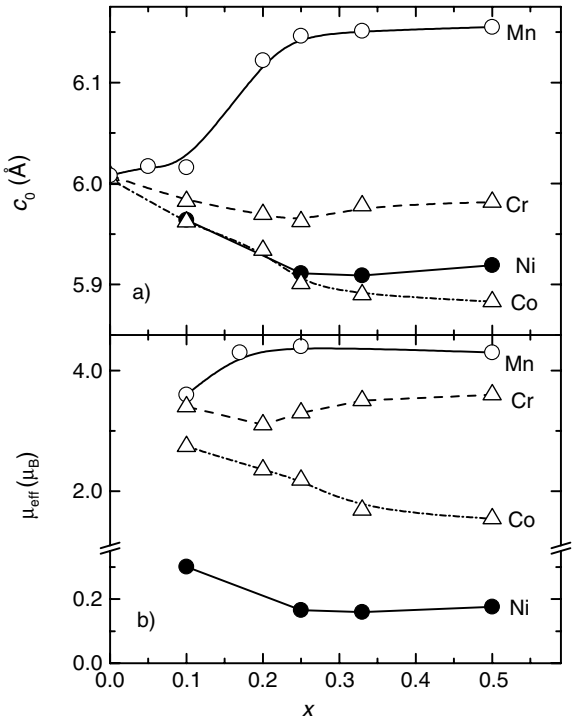

Figure 8. (a) Concentration dependences of (a) the lattice parameter c and (b) the effective magnetic moment μ_{eff} per M ion for M_xTiSe_2 systems with M = Cr, Mn, Co and Ni.

upturn of C_p/T versus T^2 dependences for Ni_xTiSe_2 when the temperature decreases below 4 K. A pronounced upturn of the C_p/T versus T^2 curves over the low-temperature range was also observed for some M_xTiS_2 in [26, 27], where different models (spin fluctuation model, Schottky contribution and others) are considered, which could be used for the explanation of such a behaviour. Further investigations are needed in order to determine the origin of this phenomena.

4. Discussion

Although the band structure calculations were made for ordered crystal structures of M_xTiX_2 compounds, one can assume that the results of these calculations are also applicable to the compounds with randomly distributed M ions in the layers between X–Ti–X trilayers. According to the calculations [18, 19], the hybridization degree as well as the position of the M 3d band is expected to depend on the type of inserted M ions. The hybridization of M 3d states with $TiSe_2$ bands should lead to a loss of the ionic character of the inserted M atoms and may result in a significant lattice distortion owing to the intercalation.

In order to reveal how the type of the M metal influences the lattice at the intercalation, we plotted in figure 8(a) the x dependence of the lattice parameter c_0 for Ni_xTiSe_2 as well as for other M_xTiSe_2 compounds intercalated by M = Cr [23], Mn [24] and Co [36]. As can be seen, the intercalation of Cr with the partially occupied majority subband, as well as the

intercalation of Co and Ni with the partially occupied minority subband, leads to a decrease in the lattice parameter c_0 with increasing intercalant content up to $x = 0.25$. The contraction of the lattice observed in the c-direction may be associated with the bonding effect arising from the formation of covalent-like links between X–Ti–X layers via intercalated M ions. Since, for M = Ni or Co, the reduction of the c_0 parameter is more significant than in the case of the Cr intercalation, one can suggest a stronger degree of hybridization of Ni and Co 3d states with Ti 3d and Se 4p states in comparison with Cr. As for the Mn_xTiSe_2 system, the increase in the c_0 parameter owing to the Mn intercalation may be indicative of a lower hybridization effect in the case of the half-filled 3d-electron band of intercalated 3d metals [24]. Further increase of the M concentration up to $x = 0.5$ is accompanied by a growth of the c_0 parameter in the case of M = Cr and Ni, while the c_0 parameter remains practically constant for M = Mn and decreases more slowly at the intercalation of Co. Such a behaviour of $c_0(x)$ in M_xTiSe_2 at $x > 0.25$ may be attributed to the saturation of the covalent-like links in these intercalated compounds [36].

In figure 8(b), we present the effective magnetic moment $\mu_{\rm eff}$ per M ion versus the concentration of inserted atoms for the same M_xTiSe_2 systems. All these data were obtained by using the expression (1) without taking into account a possible contribution from impurities in the matrix as was made in the present work. Comparison of $\mu_{\rm eff}(x)$ for M = Cr, Mn and Co with that obtained in the present work for Ni_xTiSe_2 shows that, in all these systems, the value of $\mu_{\rm eff}$ is significantly lower than that for free M ions; moreover, a pronounced correlation between $\mu_{\rm eff}(x)$ and $c_0(x)$ exists: the decrease in c_0 with an increase in intercalant content up to $x \sim 0.25$ in the case of M = Cr, Co or Ni is accompanied by a decrease of $\mu_{\rm eff}$, whereas both c_0 and $\mu_{\rm eff}$ values show growth with the intercalation of Mn over the low-concentration range. In our opinion, such a correlation indicates that the value of $\mu_{\rm eff}$ in M_xTiSe_2 compounds is controlled by the hybridization degree of the M 3d and Ti 3d states. These findings imply an itinerant nature of the magnetic moment of the M ions intercalated. The presence of the CW-type contribution in the itinerant d-electron magnets is associated with the temperature dependence of the local amplitude of spin fluctuations [40]. As additional evidence of the itinerant character of magnetism in the M_xTiX_2 compounds, one may consider the results of high-field magnetization measurements performed at low temperatures for some intercalated compounds $Cr_{0.5}TiSe_2$ [23], Cr_xTiTe_2 [25] and Fe_xTiS_2 [31]. In these compounds, the magnetic moment per intercalated guest atom in saturation, $\mu_{\rm S}$, is found to be appreciably lower than the saturation moment value calculated from the localized moment model and lower than the effective magnetic moment obtained from the paramagnetic susceptibility measurements. One can evaluate the Rhodes–Wohlfarth ratio $\mu_{\rm eff}/\mu_{\rm S}$ which is usually used for characterizing spin-fluctuation systems [40]. Taking the values of $\mu_{\rm eff} = 4.0\mu_{\rm B}$ [33] and $\mu_{\rm S} = 2.55\mu_{\rm B}$ [31], we estimated this ratio for $Fe_{0.33}TiSe_2$ as 1.56. The same value of the $\mu_{\rm eff}/\mu_{\rm S}$ ratio was obtained for the $Cr_{0.5}TiSe_2$ compound (see [23]). These data allow us to suggest that the physical properties of TiX_2 compounds intercalated by 3d metals are appreciably influenced by spin fluctuations. This assumption is supported by specific heat measurements [26] which show that the value of the electronic specific heat coefficient γ for M_xTiS_2 is appreciably enhanced in comparison with the theoretical value. Unfortunately, we did not reach a saturation of the magnetization for Ni_xTiSe_2 compounds at $T = 2$ K in the magnetic field used in the present work (50 kOe) and, therefore, we could not evaluate the $\mu_{\rm eff}/\mu_{\rm S}$ ratio in this case. Nevertheless, bearing in mind the data obtained for isostructural M_xTiX_2 compounds, one can suppose that the CW-type contribution to the total magnetic susceptibility of Ni_xTiSe_2 originates from the temperature dependence of the local amplitude of spin fluctuation in the Ni 3d-electron subsystem as well as in M_xTiX_2 compounds intercalated by other 3d metals. Despite forming a band and hybridization with Ti 3d and Se 4p electrons, the 3d electrons of inserted M atoms seem not to be fully delocalized in M_xTiSe_2. This follows from recent studies of the magnetic circular

dichroism for isostructural Fe_xTiS_2 compounds [41]. As it turned out, the total magnetic moment of Fe ions inserted into the TiS_2 matrix includes an appreciable contribution from the orbital angular momentum. This orbital contribution is found to decrease with an increase in intercalant content, which implies a change of the delocalization degree of M 3d electrons upon intercalation.

As can be seen from table 1, both the sum $(\chi_d + \chi_{p0})$ and the electronic specific heat coefficient γ for Ni_xTiSe_2 reveal an analogous behaviour for the Ni intercalation, i.e., significant growth on increasing x up to $x = 0.1$–0.25 and their non-monotonic change on further intercalation. Such a correlation seems unsurprising, since both χ_{p0} and γ are proportional to the density of electronic state at the Fermi level and may be enhanced by the contribution of spin fluctuations. There are several factors which may determine such a complicated concentration dependence of χ_{p0} and γ in Ni_xTiSe_2: (i) the disappearance of the energy gap associated with the CDW state in the parent $TiSe_2$; (ii) the formation of the additional band near the Fermi level; (iii) the appearance of an additional contribution from spin fluctuations in the 3d-electron subsystem of inserted ions; (iv) the shift of the position of the Fermi level owing to growth in the concentration of the s and d electrons which are put into $TiSe_2$; (v) variations of the Ni 3d–Ti 3d hybridization and the lattice parameters; and (vi) the change of the crystal structure at a high Ni content ($x \sim 0.5$). The increase of χ_{p0} and γ values with the Ni intercalation over a low-concentration range ($x < 0.25$) may be attributed to the first two reasons, while their further non-monotonic change with an increase in x is not understood yet. It should be noted that the value of $\chi_0(T = 0) = 1.2 \times 10^{-7}$ observed in the present work for $Ni_{0.1}TiSe_2$ is lower than that obtained from the magnetic susceptibility measurements for $M_{0.1}TiSe_2$ compounds intercalated by other 3d metals: $\chi_0 = 15 \times 10^{-7}$ for M = Mn [24]; 4.3×10^{-7} for M = Fe [36]; and 2.3×10^{-7} for M = Co [36] (all data are in emu g^{-1} Oe^{-1}). These data suggest a decrease of DOS with an increase in atomic number of the 3d metal intercalated in M_xTiSe_2, which is in agreement with band structure calculations performed for isostructural M_xTiS_2 compounds [18]. The growth of the paramagnetic contribution from conduction electrons with increasing temperature observed for all Ni_xTiSe_2 compounds (shown in the inset to figure 4) is associated with the negative sign of the coefficient P in expressions (2) and (3). Such a temperature dependence of χ_p may result from the temperature dependence of the Fermi energy. It should be noted that a strong temperature dependence of E_F was derived from the calculations [14] for $TiSe_2$ at $T > T_t$, where the magnetic susceptibility of this compound increases with an increase in temperature.

Let us consider the change in the lattice contribution to specific heat and phonon dynamics observed in Ni_xTiSe_2. At first sight, one may assume that the low-temperature specific heat for Ni_xTiSe_2 should obey the T^2 or T^n power law ($2 < n < 3$) owing to its layered crystal structure as for graphite [42]. However, because of a significantly higher value of the shearing elastic constant for $TiSe_2$ ($C_{44} = 14.3 \times 10^{10}$ dyn cm^{-2} [5]) compared with graphite (4.6×10^{10} dyn cm^{-2} [43]), this compound can be considered to be of a three-dimensional nature. Thus the low-temperature specific heat of $TiSe_2$ and Ni_xTiSe_2 should obey the T^3 law, as is observed below 7 K (figure 7). The intercalated Ni_xTiSe_2 compounds should have a higher degree of three-dimensionality owing to the bonding effect through Ni atoms. One may suggest that, at $T > 7$ K, the deviation of the experimental $C_p(T)$ curves from that calculated from the simple Debye model originates from a strong anisotropy in the acoustic modes in $TiSe_2$ [5]. The $C_p(T)$ dependence for $TiSe_2$ at higher temperatures may also be influenced by the phonon softening which was revealed in a wide temperature range around the CDW transition [12]. It should be noted that a widely used way to describe the lattice contribution to the total specific heat is to combine both the Debye term of the acoustic phonon mode and the Einstein term of the optical mode. However, this method can scarcely be applied for $TiSe_2$ in the low-temperature region,

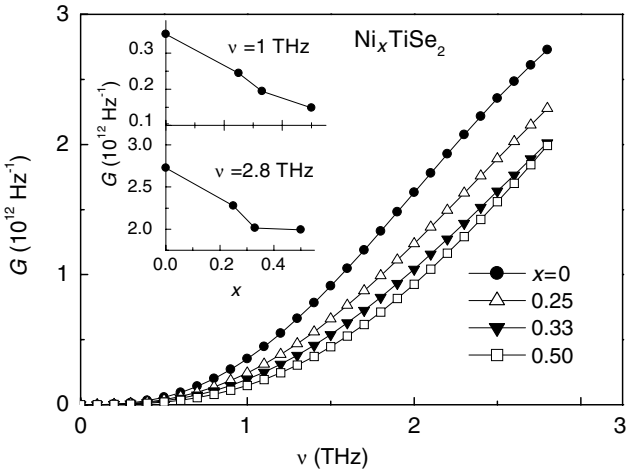

Figure 9. Phonon spectrum derived from specific heat data for Ni_xTiSe_2. Inset shows the concentration dependence of PhDOS at $\nu = 1$ and 2.8 THz.

since, as follows from the experimental data and calculations [12, 44], the contribution to the heat capacity from optical phonons should be important in this case at temperatures $\gtrsim$100 K. The change of the lattice contribution to the specific heat observed in Ni_xTiSe_2 compounds at the Ni intercalation (figure 6) may be attributed to a modification of the phonon spectrum owing to the Ni 3d–Ti 3d hybridization and formation of covalent links between Se–Ti–Se trilayers via the Ni atoms inserted. We made an attempt to obtain the phonon spectrum directly from our specific heat data for Ni_xTiSe_2 using the method proposed by Chen based on a new theorem of the Möbius inverse formula [45]. As shown in [46], by applying this method to YBCO a phonon spectrum can be obtained that agrees quite well with inelastic neutron scattering data.

The phonon contribution C_{ph} to the total specific heat of Ni_xTiSe_2 was obtained after subtraction of the electronic contribution $C_{el} = \gamma T$. Neglecting the difference between C_p and C_v, the specific heat associated with the lattice vibration can be expressed as

$$C_{ph}(T) = rk \int_0^\infty \frac{(h\nu/kT)^2 \, e^{h\nu/kT}}{(e^{h\nu/kT} - 1)^2} G(\nu) \, d\nu \tag{4}$$

where r is the number of atoms per formula unit, $G(\nu)$ is the phonon density of states (PhDOS) and other symbols have their usual meaning. For our analysis, we have chosen a low-temperature interval (up to 80 K), where the $C_{ph}(T)$ dependence is mainly determined by acoustic phonons. The $G(\nu)$ dependences calculated for Ni_xTiSe_2 compounds are presented in figure 9 for frequencies up to 3 THz which correspond to acoustic vibrations [12, 44]. In the low-frequency region, the Debye relation $G \propto \nu^2$ is found to dominate for $TiSe_2$ and for all intercalated compounds, while the value of PhDOS decreases significantly owing to the Ni intercalation. We attribute such a behaviour to stiffening of the lattice due to the bonding effect caused by the insertion of Ni atoms. The change of PhDOS with the Ni concentration at low ($\nu = 1$ THz) and high ($\nu = 2.8$ THz) frequencies is shown in insets to figure 9. As it turned out, at low frequencies, PhDOS decreases more significantly with an increase in x up to $x = 0.5$ when compared with high frequencies. The ratio of $G(x = 0)/G(x = 0.5)$ is estimated to be $\sim$2.36 for $\nu = 1$ THz, while it reaches only 1.37 for $\gamma = 2.8$ THz. Moreover, the $G(\nu)$ dependences for $x = 0.33$ and 0.5 reveal a crossover at $\nu \sim 2.8$ THz, which may be associated

with the above-discussed change of the crystal structure from the CdI_2 type at $x \leqslant 0.33$ to the monoclinic one at $x > 0.33$.

5. Conclusion

X-ray diffraction study of the crystal structure and measurements of the magnetic susceptibility and specific heat performed in the present work for the intercalated Ni_xTiSe_2 compounds have shown that the intercalation significantly modifies their main physical properties. The intercalation of Ni atoms between Se–Ti–Se trilayers substantially decreases the lattice parameter c_0 and increases the inter-atomic distances in the perpendicular direction. It has been shown that the contraction of the lattice in the c-direction is caused by a decrease of the van der Waals gap width, which is attributed to the formation of covalent links between Ni 3d and Se 4p orbitals and to the Ni 3d–Ti 3d hybridization. As follows from the phonon spectrum derived directly from the specific heat data for Ni_xTiSe_2 using the method proposed by Chen [28], the additional bonding effect and stiffening of the lattice at the Ni intercalation lead to the substantial depletion of low-frequency lattice vibrations. Inelastic neutron scattering experiments are needed to confirm this result.

A comparative analysis of the lattice and magnetic properties of Ni_xTiSe_2 compounds and other M_xTiSe_2 systems has revealed a pronounced correlation between the concentration dependence of the lattice parameter c_0 and the effective magnetic moment per M ion. The value of μ_{eff} for Ni as well as for other M metals intercalated in M_xTiSe_2 is found to be significantly lower than that expected for the free M ions. These data allow us to suggest that the value of μ_{eff} is strongly dependent on the M 3d–Ti 3d hybridization degree. The hybridization degree is suggested to increase with an increase in atomic number of the 3d metal intercalated. This suggestion is supported by the data on the Pauli paramagnetic contribution to the total magnetic susceptibility, which indicate that the DOS value at the Fermi level in M_xTiSe_2 decreases with an increase in Z. This last result may also be indicative of a shift of the position of M 3d-electron states towards low energies when the M atomic number increases. We consider all these findings as proof of the itinerant nature of the magnetic moment of 3d-transition metal ions intercalated in the $TiSe_2$ matrix. The value of the effective magnetic moment per M ion in M_xTiSe_2 is expected to be determined by the amplitude of the local spin density and spatial extension of the spin correlation [40], which are apparently dependent on the type and concentration of the M metal as well as on the hybridization degree of M 3d states with $TiSe_2$ bands.

References

[1] Motizki K (ed) 1986 *Structural Phase Transitions in Layered Transition Metal Compounds* (Boston: Reidel)
[2] Inoue M, Hughes H P and Yoffe A D 1989 *Adv. Phys.* **38** 565
[3] Wilson J A, Di Salvo F J and Mahajan S 1975 *Adv. Phys.* **24** 117
[4] Di Salvo F J, Moncton D E and Waszczak J V 1976 *Phys. Rev.* B **14** 4321
[5] Stirling W G, Dorner B, Cheeke J D N and Revelli J 1976 *Solid State Commun.* **18** 931
[6] Caillé A, Lepine Y, Jericho M H and Simpson A M 1983 *Phys. Rev.* B **28** 5454
[7] Craven R A, Di Salvo F J and Hsu F S L 1978 *Solid State Commun.* **25** 39
[8] Holy J A, Woo K C, Klein M V and Brown F C 1977 *Phys. Rev.* B **16** 3628
[9] Woo K C, Brown F C, McMillan W L, Miller R J, Schaffman M J and Sears M P 1976 *Phys. Rev.* B **14** 3432
[10] Wilson J A and Mahajan S 1977 *Commun. Phys.* **2** 23
[11] Wilson J A 1978 *Phys. Status Solidi* b **81** 11
[12] Holt M, Zschak P, Hong H, Chou M Y and Chiang T-C 2001 *Phys. Rev. Lett.* **86** 3799
[13] Kidd T E, Miller T, Chou M Y and Chiang T-C 2002 *Phys. Rev. Lett.* **88** 226402
[14] Bussmann-Holder A and Büttner H 2002 *J. Phys.: Condens. Matter* **14** 7973

[15] Kouano M, Suezava M, Watanabe H and Inoue M 1994 *J. Phys. Soc. Japan* **63** 1114
[16] Calvarin G, Gavarri J, Buhannic M, Colombet P and Danot M 1987 *Rev. Phys. Appl.* **22** 1131
[17] Tazuke Yu and Takeyama T 1997 *J. Phys. Soc. Japan* **66** 827
[18] Suzuki N, Teshima T and Motizuki K 1992 *Physics of Transition Metals* vol 1 ed O M Opreneer and J Kubler (Singapore: World Scientific) p 374
[19] Postnikov A V, Neuman M, Plogman St, Yarmoshenko Yu M, Titov A N and Kuranov A V 2000 *Comput. Mater. Sci.* **17** 450
[20] Ueda Y, Fukushima K, Negishi H, Inoue M, Taniguchi M and Suga S 1987 *J. Phys. Soc. Japan* **56** 2471
[21] Yamasaki A, Imada S, Sekiyama A, Suga S, Matsushita T, Muro T, Saitoh Y, Negishi H and Sasaki M 2002 *Surf. Rev. Lett.* **9** 961
[22] Titov A N, Kuranov A V, Pleschev V G, Yarmoshenko Yu M, Yablonskikh M V, Postnikov A V, Plogmann S, Neumann M, Ezhov A V and Kurmaev E Z 2001 *Phys. Rev.* B **63** 035106
[23] Pleschov V G, Baranov N V, Titov A N, Inoue K, Bartashevich M I and Goto T 2001 *J. Alloys Compounds* **320** 13
[24] Pleschev V G, Titov A N and Baranov N V 2002 *Fiz. Tverd. Tela* **44** 62
Pleschev V G, Titov A N and Baranov N V 2002 *Phys. Solid State* **44** 64 (Engl. Transl.)
Maksimov V I, Baranov N V, Pleschov V G and Inoue K 2004 *J. Alloys Compounds* **384** 33
[25] Pleschov V G, Korolev A V and Dorofeev U A 2004 *Fiz. Tverd. Tela* **46** 288
Pleschov V G, Korolev A V and Dorofeev U A 2004 *Phys. Solid State* **46** 289 (Engl. Transl.)
[26] Inoue M, Muneta Y, Negishi H and Sasaki M 1986 *J. Low Temp. Phys.* **63** 235
[27] Takase K, Negishi H, Sasaki M and Inoue M 1996 *J. Low Temp. Phys.* **103** 107
[28] Tazuke Y, Yoshioka T and Hoshi K 1986 *J. Magn. Magn. Mater.* **54–57** 73
[29] Negishi H, Shoube A, Takahashi H, Ueda Y, Sasaki M and Inoue M 1987 *J. Magn. Magn. Mater.* **67** 179
[30] Tazuke Y, Satoh T and Miyadai T 1987 *J. Magn. Magn. Mater.* **70** 194
[31] Negishi H, Koyano M, Inoue M, Sakakibara T and Goto T 1988 *J. Magn. Magn. Mater.* **74** 27
[32] Tazuke Y 1995 *J. Magn. Magn. Mater.* **140–144** 155
[33] Huntley D R, Stenko M J and Hiebl K J 1984 *J. Solid State Chem.* **52** 233
[34] Arnaud Y, Chevreton M, Ahouanjinou A, Danot M and Rouxel J 1976 *J. Solid State Chem.* **17** 9
[35] Larson A C and Von Dreele R B 1986 *Report LANSCE.MS-H805* Los-Alamos National Laboratory, Los-Alamos, NM 87545
[36] Kuranov A V, Pleschev V G, Titov A N, Baranov N V and Krasavin L S 2000 *Fiz. Tverd. Tela* **42** 2029
Kuranov A V, Pleschev V G, Titov A N, Baranov N V and Krasavin L S 2000 *Phys. Solid State* **42** 2089 (Engl. Transl.)
[37] Chevreton M 1967 *Bull. Soc. Fr. Minéral. Crystallogr.* **90** 592
[38] Vonsovsky S V 1971 *Magnetism* (Moscow: Nauka) (in Russian)
[39] Krasavin L S, Titov A N and Antropov V M 1998 *Fiz. Tverd. Tela* **40** 2165
Krasavin L S, Titov A N and Antropov V M 1998 *Phys. Solid State* **40** 1692 (Engl. Transl.)
[40] Morya T 1985 *Spin Fluctuations in the Itinerant Electron Magnetism* (Berlin: Springer)
[41] Yamasaki A, Imada S, Utsunomiya H, Muro T, Saitoh Y, Negishi H, Sasaki M, Inoue M and Suga S 2001 *Physica* E **10** 387
[42] Bergenlid U, Hill R W, Webb E J and Wilks J 1954 *Phil. Mag.* **45** 851
[43] Nicklow R, Wakabayashi N and Smith H G 1972 *Phys. Rev.* B **5** 4951
[44] Jaswal S S 1979 *Phys. Rev.* B **20** 5297
[45] Chen N X 1990 *Phys. Rev. Lett.* **64** 1193
[46] Dai XianXi, Tao Wen, GuiCun Ma and JiXin Dai 1999 *Phys. Lett.* A **264** 68